Reliable readout of mixture components from small populations of piriform cortical neurons

Sapir Penker, Tamar Licht, and Dan Rokni*

Department of Neurobiology, School of Medicine and IMRIC, The Hebrew University, Jerusalem, Israel

* Corresponding author: Dan Rokni

Abstract

Airborne chemicals emitted by multiple objects, mix in the air prior to reaching the nose, complicating the recognition of specific odors of interest. The olfactory system is therefore faced with the task of identifying objects in the presence of rich and often unpredictable backgrounds. Piriform cortex is thought to be the site of object recognition and scene segmentation, yet the nature of its responses to odorant mixtures is largely unknown. In this study we asked two related questions. 1) How do mixture representations relate to the representations of mixture components? And 2) Can the identity of mixture components be readout from mixture representations in piriform cortex? To answer these question, we recorded single unit activity in the piriform cortex of naïve mice while sequentially presenting single odorants and their mixtures. We find that the magnitude of piriform cortical responses increases with added mixture components, and that the responses of individual neurons are well explained by a normalization model. Finally, we show that mixture components can be identified from piriform cortical activity by pooling responses of a small population of neurons. These results suggest that piriform cortical representations are well suited to perform figure-background segmentation without the need for learning.

Introduction

Odors in the mammalian olfactory system, are encoded by sensory neurons in the olfactory epithelium, each expressing a single olfactory receptor gene (Axel, 1995). Each odorant may activate multiple olfactory receptors and each olfactory receptor can be activated by a variety of odorants (Abaffy et al., 2006; Araneda et al., 2000; Grosmaitre et al., 2009; Kajiya et al., 2001; Malnic et al., 1999; Rubin and Katz, 1999; Soucy et al., 2009). Epithelial representations are projected to the olfactory bulb where individual principal neurons (mitral and tufted cells), primarily represent the activation of a single type of olfactory receptor (Tan et al., 2010). This mostly labeled-line processing is broken in the projection of olfactory bulb representations onto piriform cortex. There, individual cortical neurons integrate inputs from mitral and tufted cells representing multiple receptor channels and individual mitral and tufted cells project diffusely across piriform cortex (Apicella et al., 2010; Ghosh et al., 2011; Miyamichi et al., 2011; Sosulski et al., 2011). The integration of receptor channel information by individual neurons in piriform cortex, underlies its proposed role in object recognition (Gottfried, 2010; Thomas-Danguin et al., 2014; Wilson and Sullivan, 2011). Because individual objects often emit hundreds of volatile chemicals, of which some may also be emitted from other objects, object recognition relies on the integration of information from multiple olfactory receptor channels. The finding that piriform neurons indeed require the activation of odorant receptor-combinations to respond, provided further support for the view that piriform cortex is the site of object recognition (Davison and Ehlers, 2011).

In natural environments, object recognition is complicated by the mixing of odorants from multiple objects. A single sniff will typically introduce hundreds to thousands of volatile chemicals originating from multiple sources into the nose. To be able to recognize an object, the olfactory system must therefore segment odors from their background (Grabska-Barwińska et al., 2017; Kadohisa and Wilson, 2006a; Li and Hertz, 2000; Linster et al., 2007; Mathis et al., 2016; Rokni and Murthy, 2014; Rokni et al., 2014; Vinograd et al., 2017). Cross-odorant interactions at different levels of the olfactory system further complicate object recognition by creating mixture representations that are not linear combinations of the individual component representations. Already at the level of the olfactory epithelium, odorants may interact non-linearly, typically antagonistically (Duchamp-Viret et al., 2003; Kurahashi et al., 1994; Oka et al., 2004; Takeuchi et al., 2009; Xu et al., 2019; Zak et al., 2019). While these interactions make odorant representations highly background dependent, they may actually increase the amount of information carried by a population of sensory neurons about mixture components (Reddy et al., 2018). At the level of the olfactory bulb, lateral inhibitory circuits may further modify odor representations in a background dependent manner (Arevian et al., 2008; Aungst et al., 2003; Fantana et al., 2008; Urban, 2002; Yokoi et al., 1995), however intraglomerular circuits seem to be the main player in shaping olfactory bulb output (McGann et al., 2005). Piriform cortex integrates these non-linear odor representations from the olfactory bulb and is thought to utilize local recurrent circuitry to generate representations that allow for object recognition (Bolding and Franks, 2018; Franks et al., 2011; Miura et al., 2012; Poo and Isaacson, 2009, 2011; Roland et al., 2017; Suzuki and Bekkers, 2012). Currently however, the nature of these mixture representations in piriform cortex is poorly understood. Specifically, how do mixture representations relate to the single component representations (in other words, can one predict a piriform cortical neuron's response to a mixture based on knowledge of the individual component responses)? And how can information about mixture components be readout from piriform cortical mixture representations?

To answer these questions, we systematically characterized mixture representations in piriform cortex in anesthetized mice in vivo, challenging each neuron with all possible combinations from sets of 4 odorants. We found that most responses can be well explained by a model that assumes normalization. We used receiver operator characteristic (ROC) analysis (Green and Swets, 1966), and linear classifiers (Rosenblatt, 1958), to analyze how informative single neurons and neuronal populations are for identifying specific odorants from mixtures. We find that pooling information from a relatively small number of neurons enabled almost complete identification of mixture components.

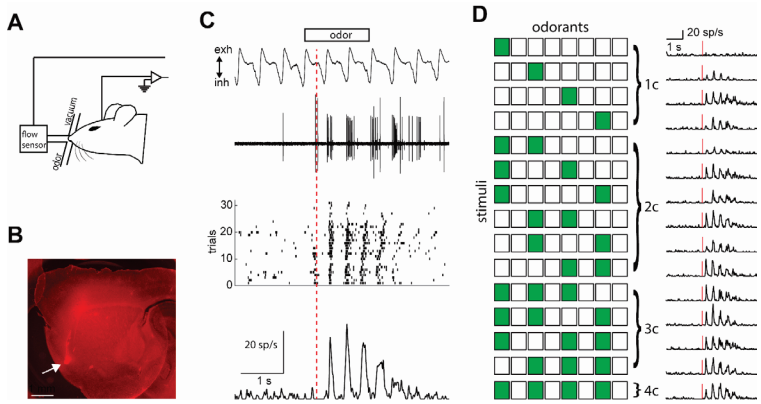

Figure 1. Mixture responses in piriform cortex. **A.** Schematic of experimental setup. **B.** Sagittal section of a brain that was injected with a 10Kd rhodamine-labeled dextran at the same coordinates used for recordings. Arrow marks the injection site in the anterior piriform cortex. **C.** Example raw data, raster plot, and PSTH in response to a mixture of 2 odorants (3&5). **D.** Responses of the same cell shown in C to all combinations of 4 odorants.

Results

We recorded the responses of single neurons in the anterior piriform cortex of naïve anesthetized mice, to all possible combinations of 4 odorants (4 single odorants, 6 pairs, 4 triplets, 1 mix of 4, Figure 1). Various sets of 4 odorants were used (from 8 odorants available in the odor presentation machine). Dye injections in the same coordinates that were used for recordings (1.5 mm anterior and 2.8 mm lateral to bregma), verified piriform cortical targeting (Figure 1B). Odor stimuli were presented using a mask that fit the mouse's snout and were cleared with constant negative pressure (Figure 1A). The mask was also connected to a mass flow sensor for continuous monitoring of respiration. We recorded from 53 neurons that responded significantly to at least one of the 15 odor combinations. Responses were typically strongly modulated by respiration as was previously shown in awake rats (Figure 1C,D) (Miura et al., 2012), and were predominantly positive (increases in firing rate) with only 18% showing mild decreases in firing rate (Figure 2A). This may be an underestimate of inhibitory responses as most neurons had a basal firing rate of less than 1 spike per second, rendering our analysis less sensitive to inhibition. Of the responding neurons, most responded significantly to more than one of the individual odorants (Figure 2B). We analyzed response statistics across all recorded neurons, to assess the overall responsivity of piriform cortex to mixtures with increasing numbers of components. The fraction of significant responses ($p<0.01$, Wilcoxon ranksum test) was positively correlated with the number of mixture components ($r=0.98$, $p=0.017$, Figure 2C). The average firing rate in a 3 second response period was also positively correlated

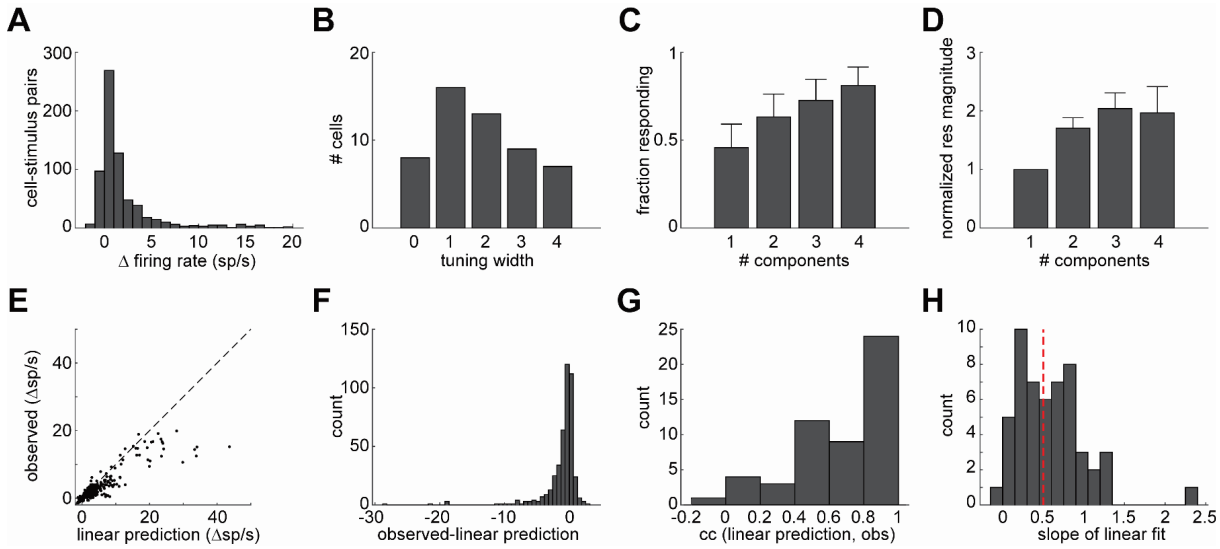

Figure 2. Population response statistics. **A.** histogram of the changes in firing rates obtained for all cell-odor responses. **B.** Histogram of the tuning widths of all cells that responded to at least one of the fifteen stimuli. Tuning width is defined as the number of single odorants that elicited a statistically significant response ($p<0.01$). **C.** Fraction of significant responses ($p<0.01$) as a function of the number of odorants in the mixture. **D.** Normalized responses (change in firing rate) vs the number of odorants in the mixture. For each cell, we normalized all responses to the mean response to the 4 single odorants. **E.** observed responses vs the linear sum of individual odorant responses (LP). Responses of all cell-mixture pairs are shown. **F.** Histogram of the differences between observed and linearly predicted mixture responses. **G.** Histogram of correlation coefficients between the linearly predicted and observed responses. **H.** Histogram of the slopes obtained in linear fits to the relationship between the linearly predicted and observed responses. Red dashed line indicates the median.

with the number of mixture components, although potentially showing saturation above 3 components (r=0.88, p=0.12, Figure 2D). To relate mixture responses to individual component responses, we compared mixture responses of each neuron to the linear sum of the responses to individual mixture components (Figure 2E). Responses were taken as the mean firing rate during a 3 second response period. Most mixture responses were below the linear prediction (Figure 2E,F). These analyses indicate that cortical responses increase with increasing numbers of mixture components at the population level. To analyze the effect of adding mixture components on individual neuron responses, we calculated the correlation coefficient between the linearly predicted responses and the actual mixture responses, for each neuron. Linear prediction was calculated as the sum of single component responses. 52/53 neurons (98%) showed a positive correlation and 39/53 neurons (74 %) showed a correlation coefficient above 0.5 (Figure 2G). Linear fits were used to assess the average slope of the relationship between the linear sum of individual odorant responses and mixture responses. The median slope of the linear fits was 0.5 (Figure 2H). These analyses show that the vast majority of individual piriform cortical neuron responses to odorant mixtures increase with added mixture components and that this increase is typically, sub-linear.

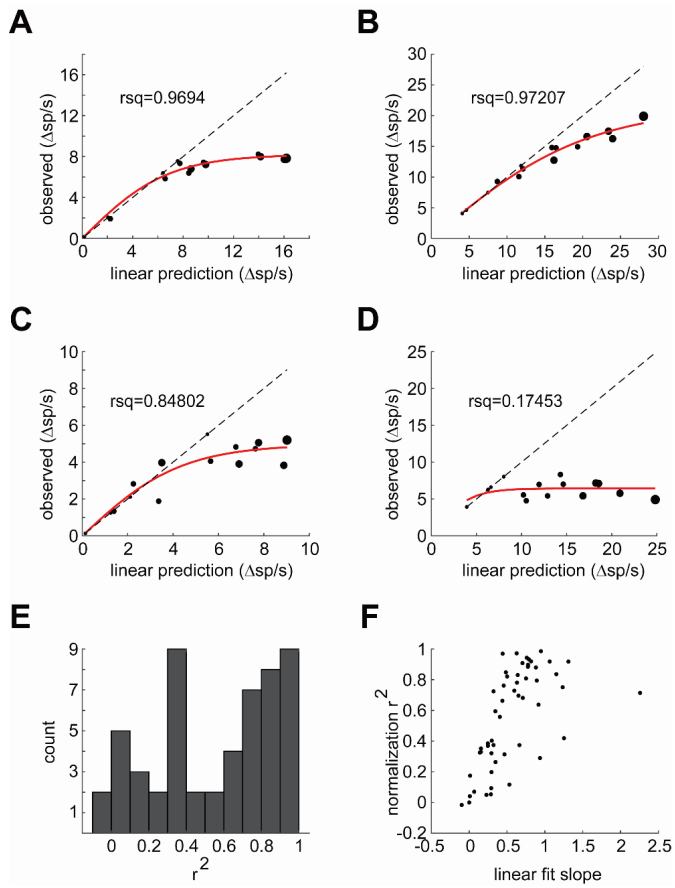

Figure 3. Normalization model for piriform mixture responses. **A-D.** Examples from 4 cells showing the relationship between the linearly predicted and observed responses. The size of the symbol indicates the number of odorants in the mixture. Red line shows the fit to equation 1. Dashed line is the unity line. **E.** Histogram of the coefficients of determination (r^2) of the fits to equation 1 obtained from all cells. **F.** The coefficients of determination plotted against the slope of a linear fit.

While linear fits were useful as a minimal model for analyzing the general increase in piriform responses with added components, neuron's firing rates are limited by their intrinsic properties and by inhibitory inputs, and therefore cannot increase linearly with the linear prediction. Indeed, piriform cortical odor representations have been shown to be strongly affected by local inhibitory circuits that perform a computation akin to normalization (Bolding and Franks, 2018). We therefore fitted mixture responses with a model that is similar to that was used to describe mixture responses in olfactory sensory neurons (Mathis et al., 2016):

$$R = Rmax\left(\frac{2}{1+e^{-s\cdot LP}} - 1\right) \qquad (eq.1)$$

In this model, R is the neuron's response to a mixture, LP is the linear sum of the individual component responses, Rmax is the neuron's maximal response, and s is a parameter that sets the slope of the function at LP=0. Rmax and s are the two fitted parameters. We found that this model explains mixture responses well for most neurons (Figure 3A-C). Some neurons however, could not be properly explained with such a model (Figure 3D). The normalization model could account for most of the variance (r^2 above 0.5) in 30/53 (57 %) of the cells (Figure 3E). The neurons that could not be well explained with this model showed little increase in their responses as mixture components were added as assessed by the slope of the linear fit (Figure 3F). Whether these neurons represent a separate neuronal subtype is unclear. These results indicate that piriform neuronal responses grow monotonically with mixture richness and that these responses can often be explained by a simple normalization model.

One of the suggested tasks for piriform cortex is that of figure-background segregation. It was recently suggested that individual piriform neurons may be able to detect target odors in a background invariant manner by pooling inputs from multiple glomeruli (Mathis et al., 2016). We therefore asked whether and how the presence of individual odorants in mixtures can be extracted from the activity of individual piriform neurons. We used receiver operator characteristic (ROC) analysis to test whether the responses to mixtures that contain a specific odorant are discriminable from responses to mixtures that do not contain the same odorant (Figure 4). For each neuron, we assessed discriminability for all 4 odorants in the experiment and quantified it with the area under the ROC curve (auROC). We assessed each neuron's discrimination power with its best discriminated odorant (Figures 4A-B). Many neurons yielded high levels of discriminability with 11/53 (21%) cells having an auROC of above 0.8. The discriminability for each odorant based on its single best neuron ranged from auROC of 57 to 99.7 and averaged at 79 (Figure 4C). This analysis indicates that single piriform neurons may be highly informative about the presence of a target odorant within a mixture.

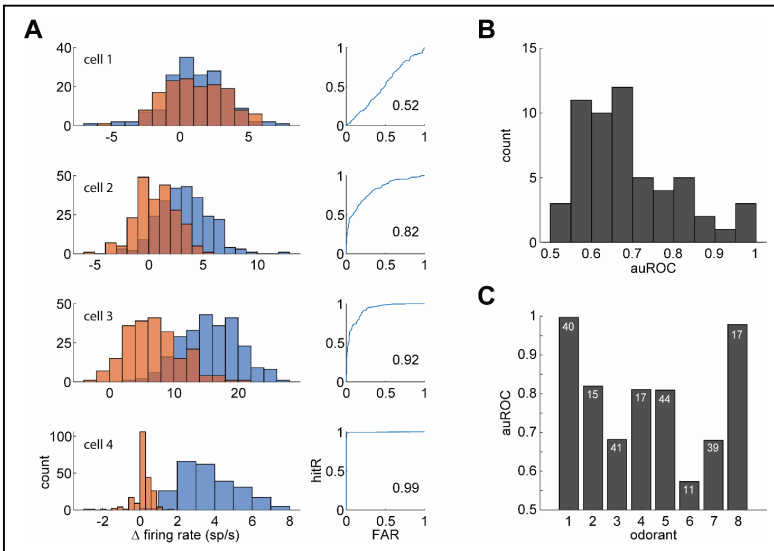

Figure 4. Detection of target odorants with single neurons. **A.** The ROC analysis of 4 example cells. Firing rate histograms are shown on left (blue – all mixtures including a particular odorant, red – all mixtures excluding the odorant). Panels on the right show hit rate vs false alarm rate as the decision boundary is shifted (numbers indicate the area under the curve). **B.** Histogram of the area under the ROC curve. The highest value for each cell (across the 4 odorants) is included. **C.** The maximal area under the curve obtained for each odorant. The number of neurons tested with each odorant is indicated.

We next analyzed the ability to detect target odorants from the activity of piriform cortical populations (Figure 5). We pooled data from all cells recorded using a specific set of 4 odorants (37 cells) to create a pseudo-population. We then trained a linear classifier (realized as a logistic regression) to classify these trials according to the presence of each individual odorant, using a separate classifier for each odorant. To avoid over fitting, classifiers were cross validated by constructing a test set that included a single response to each of the 15 odor combinations. Test set responses were not included in the training set. The mean classification accuracy across target odorants was 88 % correct (99% for odorant 1, 88% for odorant 2, 86% for odorant 3, and 78% for odorant 4). The performance of these classifiers typically decreased for richer mixtures, starting from an average performance of 94% for single odorants and decreasing to 85% for mixtures with 4 components (Figure 5A). To assess the number of neurons required to detect individual odorants from mixtures, we trained classifiers using sub populations (Figure 5B). We started with the entire population and following each iteration removed the neuron with the minimal absolute weight. On average, 5 neurons were sufficient to reach a performance level above 90 % of the level achieved with the entire population (defined relative to chance level, 1 neuron for odorant 1, 7 for odorant 2, 8 for odorant 3, and 5 for odorant 4). These analyses show that the detection of target odorants against background mixtures can be reliably achieved with a small number of piriform neurons.

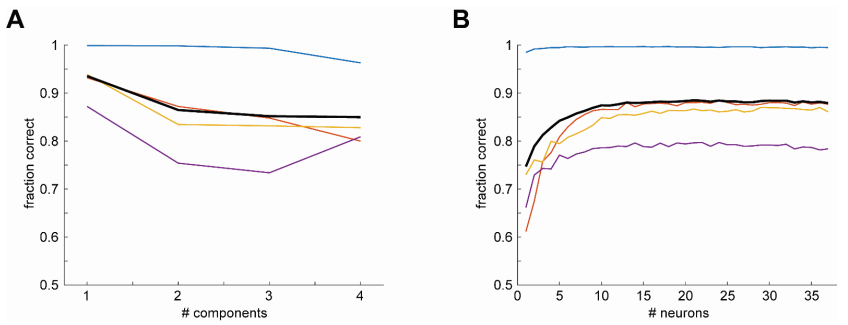

Figure 5. Detection of target odorants with pseudo-populations. **A.** Performance of the classifiers based on the entire population of neurons as a function of the number of odorants in the mixture. Colored lines show the performance for each of the four odorants and black line shows the average performance across odorants. **B.** Performance of a linear classifier as a function of population size. Colored lines show the performance for each of the four odorants and black line shows the average performance across odorants.

Discussion

We recorded from single neurons in the piriform cortex of anesthetized mice and describe their responses to odorant mixtures. We used receiver operator characteristic (ROC) analysis, and linear classifiers to describe the availability of information regarding mixture components in single neuron, and population activity, respectively. Our main findings are that (i) piriform response magnitude (number of cells responding, and number of spikes generated) increases when additional components are added to the mixture, (ii) responses of individual neurons can be described with a normalization model that relates mixture responses to the linear sum of individual component responses, (iii) individual odorants can be reliably detected from mixtures by the firing of small neuronal populations in piriform cortex.

Our finding that response magnitude is increased when mixture components are added may seem expected at first, however recent studies have suggested that response magnitude may be almost

independent of the stimulus, due to an extreme contribution of inhibition to odor responses in piriform cortex (Bolding and Franks, 2018; Stettler and Axel, 2009). Anecdotal measurement of piriform responses to pairs of odorants, using calcium imaging found that while some neurons respond only to the combination of 2 odorants, others respond only to single odorants (Stettler and Axel, 2009). Notably, these findings were also observed under anesthesia. Using a large number of odorant combinations, we were able to show that most neurons indeed increase their responses when mixture components are added. Another study analyzed the responses of piriform cortical neurons to increasing concentrations of odorants and found that extreme normalization maintains cortical responses at a rather constant level (Bolding and Franks, 2018). The difference between the level of normalization found in response to varying concentrations of an individual odorant compared to the level of normalization that we find here is intriguing. It is plausible that the level of normalization depends on the amount of overlap in the glomerular representations of mixture components which may be maximal for the case of increasing concentrations. Some relationship between odorant structure similarities and mixture representations has indeed been suggested (Yoshida and Mori, 2007).

We found that responses of most piriform neurons were well explained by a normalization model. Normalization has been found in many cortical regions and has been proposed as a canonical computation performed by cortical circuits that allows them to encode variables monotonically without saturating (Carandini and Heeger, 2012). Normalization was also demonstrated in the drosophila antennal lobe, the insect brain region equivalent to the mammalian olfactory bulb (Olsen et al., 2010). While most neurons were well fit by the normalization model, it is important to note that some neurons were not. These cells were mostly cells that did not increase their activity with increased numbers of mixture components, and it is possible that we only probed them with stimuli that push them to saturated response levels. However, these may actually be a separate population of neurons that integrate mixture components differently. Indeed principal neurons in piriform cortex include subpopulations that differ in their localization across layers, biophysical properties, projection targets, and possibly tuning width (Diodato et al., 2016; Suzuki and Bekkers, 2006, 2011; Zhan and Luo, 2010).

The finding that single piriform neurons may be sufficient to detect target odorants against background mixtures is in line with a recently proposed model that performed this classification using glomerular inputs (Mathis et al., 2016). This study showed that individual glomeruli are not informative about the presence of any specific odorant, but that pooling information from a population of glomeruli, supports accurate classification. As piriform neurons receive inputs from multiple receptor channels, they are poised to be suitable for this classification. The mice we recorded from were naïve to the odorants and were never trained to detect any of them. The fact that piriform cortical neurons in naïve mice already show an impressive ability in target detection suggests that this ability requires little or no learning. It is important to note that we challenged neurons in this set of experiments with mixtures containing up to 4 odorants. Single neuron based classification accuracy may be lower for richer mixtures. Using linear classifiers, we showed that target odorant detection can be greatly improved by pooling inputs from a small population of neurons, indicating that indeed individual neuron responses in piriform cortex are highly informative in detecting target odors against backgrounds.

In this study we focused on the ability to detect mixture components, however, mixtures of odorants that are emitted from individual objects typically create a unified percept in which the individual components are not identified (Barnes et al., 2008; Gottfried, 2010; Howard and Gottfried, 2014; Jinks and Laing, 2001;

Kadohisa and Wilson, 2006b; Wilson and Sullivan, 2011). It will be interesting for future studies to investigate how normalized mixture representations support unified object percepts.

Experimental procedures:

All experimental procedures were performed using approved protocols in accordance with institutional (Hebrew University IACUC) and national guidelines.

Data acquisition: Young adult c57bl6 male mice (10-14 weeks old, Envigo) were anesthetized (Ketamine/Medetomidine 100 and 1 mg/kg, respectively), and were restrained in a stereotaxic device (Model 940, David Kopf Instruments). The skin was removed from the scalp and a small craniotomy was made over the anterior piriform cortex (1.5 mm anterior and 2.8 mm lateral to bregma). A metal plate was attached to the skull with dental acrylic and was used to hold mice at the electrophysiological rig. Normal body temperature (37 C) was maintained with a heating pad (Harvard Apparatus). A single tungsten electrode (A-M systems, 10-12 MOhm) was lowered into the piriform cortex with a micromanipulator (Sutter Instruments). Signals from the electrode were band pass filtered (300-5000 Hz), and amplified (X1000, A-M systems 1800), and were sampled at 20KHz and digitized with 16-bit precision (National Instruments PCIe-6351). All analog signals were displayed and saved for offline analysis using custom-made software in LabVIEW (National Instruments). Injections of a TRITC-labeled 10Kd dextran (500 nL, Molecular probes cat#D1817, 10mg/ml) were used to verify piriform cortical targeting.

Odors were presented using a custom-made, computer controlled, odor presentation machine that maintains constant flow and allows mixing of odors without mutual dilution (Rokni et al., 2014). The following 8 odorants were used (all from Sigma Aldrich, CAS numbers in parentheses): 1. isobutyl propionate (540-42-1), 2. 2-ethyl hexanal (123-05-7), 3. ethyl valerate (539-82-2), 4. propyl acetate (109-60-4), 5. isoamyl tiglate (41519-18-0), 6. penethyl tiglate (55719-85-2), 7. citral (5392-40-5), 8. ethyl propionate (105-37-3). All odorants were diluted to 10% in diethyl phthalate (84-66-2), and then further diluted 8 fold in air. Odors were presented into a mask that fit the mouse's snout at a rate of 1 l/min and were cleared from the mask by vacuum that was set to create an outward flow of 1 l/min (Figure 1A). A third port of the mask was connected to a mass flow sensor (Honeywell AWM3300) to monitor respiration. For each recording session, a set of 4 odorants was chosen (initially randomly and later fixed to odorants 1, 3, 5, and 7). All 15 combinations of these 4 odorants were then presented with randomized order (typically repeating ~30 times each). Odors were presented for 1.5 s with an inter-trial interval of 20 s.

Data analysis: Action potentials were detected offline using custom-written code in Matlab. Detected spikes were then sorted using MClust (David Redish). Only units that had less than 1 in 1000 spikes to have occurred within a 3 ms refractory period were considered as single units and further analyzed. Respiratory signals were low-pass filtered with a moving average window of 250 ms. Inhalation onsets were defined as zero crossings with negative slope. All neural responses were aligned to the first inhalation onset following odor onset. PSTHs were generated with 1 ms bins and filtered with a 50 ms window Gaussian moving average. Response significance was tested by comparing inhalation aligned spike counts during a 3 second response period to inhalation aligned spike counts in a 3 second period with no odor, using the Wilcoxon ranksum test with a threshold p-value of 0.01. All responses are shown as baseline-subtracted

spike rates. To fit normalization models, data was fit to equation 1 using the lsqcurvefit function in Matlab. Fit quality was assessed with the coefficient of determination (r^2).

Receiver operating characteristic (ROC) analysis was done using the perfcurve function in Matlab. For each neuron, ROC analysis was performed separately to test the detectability of each odorant. The reported performance of each neuron is the best across the 4 odorants. The performance reported for each odorant is the best across all neurons.

For population analysis, we generated a pseudo-population by pooling neurons from different experiments in which we used the same 4 odors. Linear classifiers were realized as logistic regressions and were fit using the fitclinear function in Matlab. Classifiers were cross validated using the leave-one-out method. The reported performance for the classifiers is the mean over 1000 iterations. In each iteration a test set was generated by randomly selecting a response from each neuron to each of the 15 odor combinations. A training set that did not include the testing trials was then generated by randomly selecting trials from each neuron for each odor combination. The training set included 100 trials of each of the 15 stimuli. For assessing the effect of population size on classification accuracy, we gradually removed inputs from the classifier by sequentially removing the neuron with the minimal absolute weight.

Acknowledgements

This work was funded by a European Research Council Starting Grant (755764 - COFBMIX). We are grateful to Yoram Ben-shaul, Mati Joshua, and Ithai Rabinowitch for commenting on early versions of the manuscript, and to members of the Rokni lab for stimulating discussions.

Competing interests

The authors declare no competing financial interests.

References

Abaffy, T., Matsunami, H., and Luetje, C.W. (2006). Functional analysis of a mammalian odorant receptor subfamily. Journal of Neurochemistry *97*, 1506–1518.

Apicella, A., Yuan, Q., Scanziani, M., and Isaacson, J.S. (2010). Pyramidal cells in piriform cortex receive convergent input from distinct olfactory bulb glomeruli. J. Neurosci. *30*, 14255–14260.

Araneda, R.C., Kini, A.D., and Firestein, S. (2000). The molecular receptive range of an odorant receptor. Nat Neurosci *3*, 1248–1255.

Arevian, A.C., Kapoor, V., and Urban, N.N. (2008). Activity-dependent gating of lateral inhibition in the mouse olfactory bulb. Nat Neurosci *11*, 80–87.

Aungst, J.L., Heyward, P.M., Puche, A.C., Karnup, S.V., Hayar, A., Szabo, G., and Shipley, M.T. (2003). Centre–surround inhibition among olfactory bulb glomeruli. Nature *426*, 623–629.

Axel, R. (1995). The molecular logic of smell. Sci. Am. *273*, 154–159.

Barnes, D.C., Hofacer, R.D., Zaman, A.R., Rennaker, R.L., and Wilson, D.A. (2008). Olfactory perceptual stability and discrimination. Nat Neurosci *11*, 1378–1380.

Bolding, K.A., and Franks, K.M. (2018). Recurrent cortical circuits implement concentration-invariant odor coding. Science *361*, eaat6904.

Carandini, M., and Heeger, D.J. (2012). Normalization as a canonical neural computation. Nat Rev Neurosci *13*, 51–62.

Davison, I.G., and Ehlers, M.D. (2011). Neural circuit mechanisms for pattern detection and feature combination in olfactory cortex. Neuron *70*, 82–94.

Diodato, A., Ruinart de Brimont, M., Yim, Y.S., Derian, N., Perrin, S., Pouch, J., Klatzmann, D., Garel, S., Choi, G.B., and Fleischmann, A. (2016). Molecular signatures of neural connectivity in the olfactory cortex. Nature Communications *7*, 12238.

Duchamp-Viret, P., Duchamp, A., and Chaput, M.A. (2003). Single olfactory sensory neurons simultaneously integrate the components of an odour mixture. European Journal of Neuroscience *18*, 2690–2696.

Fantana, A.L., Soucy, E.R., and Meister, M. (2008). Rat Olfactory Bulb Mitral Cells Receive Sparse Glomerular Inputs. Neuron *59*, 802–814.

Franks, K.M., Russo, M.J., Sosulski, D.L., Mulligan, A.A., Siegelbaum, S.A., and Axel, R. (2011). Recurrent Circuitry Dynamically Shapes the Activation of Piriform Cortex. Neuron *72*, 49–56.

Ghosh, S., Larson, S.D., Hefzi, H., Marnoy, Z., Cutforth, T., Dokka, K., and Baldwin, K.K. (2011). Sensory maps in the olfactory cortex defined by long-range viral tracing of single neurons. Nature *472*, 217–220.

Gottfried, J.A. (2010). Central mechanisms of odour object perception. Nat Rev Neurosci *11*, 628–641.

Grabska-Barwińska, A., Barthelmé, S., Beck, J., Mainen, Z.F., Pouget, A., and Latham, P.E. (2017). A probabilistic approach to demixing odors. Nat Neurosci *20*, 98–106.

Green, D.M., and Swets, J.A. (1966). Signal Detection Theory and Psychophysics (New York: John Wiley & Sons, Inc.).

Grosmaitre, X., Fuss, S.H., Lee, A.C., Adipietro, K.A., Matsunami, H., Mombaerts, P., and Ma, M. (2009). SR1, a Mouse Odorant Receptor with an Unusually Broad Response Profile. J. Neurosci. *29*, 14545–14552.

Howard, J.D., and Gottfried, J.A. (2014). Configural and Elemental Coding of Natural Odor Mixture Components in the Human Brain. Neuron *84*, 857–869.

Jinks, A., and Laing, D.G. (2001). The analysis of odor mixtures by humans: evidence for a configurational process. Physiol. Behav. *72*, 51–63.

Kadohisa, M., and Wilson, D.A. (2006a). Olfactory Cortical Adaptation Facilitates Detection of Odors Against Background. Journal of Neurophysiology *95*, 1888–1896.

Kadohisa, M., and Wilson, D.A. (2006b). Separate encoding of identity and similarity of complex familiar odors in piriform cortex. Proceedings of the National Academy of Sciences *103*, 15206–15211.

Kajiya, K., Inaki, K., Tanaka, M., Haga, T., Kataoka, H., and Touhara, K. (2001). Molecular Bases of Odor Discrimination: Reconstitution of Olfactory Receptors that Recognize Overlapping Sets of Odorants. J. Neurosci. *21*, 6018–6025.

Kurahashi, T., Lowe, G., and Gold, G.H. (1994). Suppression of odorant responses by odorants in olfactory receptor cells. Science *265*, 118–120.

Li, Z., and Hertz, J. (2000). Odour recognition and segmentation by a model olfactory bulb and cortex. Network *11*, 83–102.

Linster, C., Henry, L., Kadohisa, M., and Wilson, D.A. (2007). Synaptic adaptation and odor-background segmentation. Neurobiology of Learning and Memory *87*, 352–360.

Malnic, B., Hirono, J., Sato, T., and Buck, L.B. (1999). Combinatorial Receptor Codes for Odors. Cell *96*, 713–723.

Mathis, A., Rokni, D., Kapoor, V., Bethge, M., and Murthy, V.N. (2016). Reading Out Olfactory Receptors: Feedforward Circuits Detect Odors in Mixtures without Demixing. Neuron *91*, 1110–1123.

McGann, J.P., Pírez, N., Gainey, M.A., Muratore, C., Elias, A.S., and Wachowiak, M. (2005). Odorant Representations Are Modulated by Intra- but Not Interglomerular Presynaptic Inhibition of Olfactory Sensory Neurons. Neuron *48*, 1039–1053.

Miura, K., Mainen, Z.F., and Uchida, N. (2012). Odor representations in olfactory cortex: distributed rate coding and decorrelated population activity. Neuron *74*, 1087–1098.

Miyamichi, K., Amat, F., Moussavi, F., Wang, C., Wickersham, I., Wall, N.R., Taniguchi, H., Tasic, B., Huang, Z.J., He, Z., et al. (2011). Cortical representations of olfactory input by trans-synaptic tracing. Nature *472*, 191–196.

Oka, Y., Omura, M., Kataoka, H., and Touhara, K. (2004). Olfactory receptor antagonism between odorants. The EMBO Journal *23*, 120–126.

Olsen, S.R., Bhandawat, V., and Wilson, R.I. (2010). Divisive normalization in olfactory population codes. Neuron *66*, 287–299.

Poo, C., and Isaacson, J.S. (2009). Odor Representations in Olfactory Cortex: “Sparse” Coding, Global Inhibition, and Oscillations. Neuron *62*, 850–861.

Poo, C., and Isaacson, J.S. (2011). A Major Role for Intracortical Circuits in the Strength and Tuning of Odor-Evoked Excitation in Olfactory Cortex. Neuron *72*, 41–48.

Reddy, G., Zak, J.D., Vergassola, M., and Murthy, V.N. (2018). Antagonism in olfactory receptor neurons and its implications for the perception of odor mixtures.

Rokni, D., and Murthy, V.N. (2014). Analysis and Synthesis in Olfaction. ACS Chem. Neurosci.

Rokni, D., Hemmelder, V., Kapoor, V., and Murthy, V.N. (2014). An olfactory cocktail party: figure-ground segregation of odorants in rodents. Nat Neurosci *17*, 1225–1232.

Roland, B., Deneux, T., Franks, K.M., Bathellier, B., and Fleischmann, A. (2017). Odor identity coding by distributed ensembles of neurons in the mouse olfactory cortex. ELife *6*, e26337.

Rosenblatt, F. (1958). The perceptron: A probabilistic model for information storage and organization in the brain. Psychological Review *65*, 386–408.

Rubin, B.D., and Katz, L.C. (1999). Optical Imaging of Odorant Representations in the Mammalian Olfactory Bulb. Neuron *23*, 499–511.

Sosulski, D.L., Bloom, M.L., Cutforth, T., Axel, R., and Datta, S.R. (2011). Distinct representations of olfactory information in different cortical centres. Nature *472*, 213–216.

Soucy, E.R., Albeanu, D.F., Fantana, A.L., Murthy, V.N., and Meister, M. (2009). Precision and diversity in an odor map on the olfactory bulb. Nat. Neurosci. *12*, 210–220.

Stettler, D.D., and Axel, R. (2009). Representations of odor in the piriform cortex. Neuron *63*, 854–864.

Suzuki, N., and Bekkers, J.M. (2006). Neural Coding by Two Classes of Principal Cells in the Mouse Piriform Cortex. J. Neurosci. *26*, 11938–11947.

Suzuki, N., and Bekkers, J.M. (2011). Two layers of synaptic processing by principal neurons in piriform cortex. J. Neurosci. *31*, 2156–2166.

Suzuki, N., and Bekkers, J.M. (2012). Microcircuits Mediating Feedforward and Feedback Synaptic Inhibition in the Piriform Cortex. J. Neurosci. *32*, 919–931.

Takeuchi, H., Ishida, H., Hikichi, S., and Kurahashi, T. (2009). Mechanism of olfactory masking in the sensory cilia. The Journal of General Physiology *133*, 583–601.

Tan, J., Savigner, A., Ma, M., and Luo, M. (2010). Odor Information Processing by the Olfactory Bulb Analyzed in Gene-Targeted Mice. Neuron *65*, 912–926.

Thomas-Danguin, T., Sinding, C., Romagny, S., El Mountassir, F., Atanasova, B., Le Berre, E., Le Bon, A.-M., and Coureaud, G. (2014). The perception of odor objects in everyday life: a review on the processing of odor mixtures. Front Psychol *5*.

Urban, N.N. (2002). Lateral inhibition in the olfactory bulb and in olfaction. Physiology & Behavior *77*, 607–612.

Vinograd, A., Livneh, Y., and Mizrahi, A. (2017). History-Dependent Odor Processing in the Mouse Olfactory Bulb. J. Neurosci. *37*, 12018–12030.

Wilson, D.A., and Sullivan, R.M. (2011). Cortical processing of odor objects. Neuron *72*, 506–519.

Xu, L., Li, W., Voleti, V., Hillman, E.M.C., and Firestein, S. (2019). Widespread Receptor Driven Modulation in Peripheral Olfactory Coding. BioRxiv 760330.

Yokoi, M., Mori, K., and Nakanishi, S. (1995). Refinement of odor molecule tuning by dendrodendritic synaptic inhibition in the olfactory bulb. Proc Natl Acad Sci U S A *92*, 3371–3375.

Yoshida, I., and Mori, K. (2007). Odorant Category Profile Selectivity of Olfactory Cortex Neurons. J. Neurosci. *27*, 9105–9114.

Zak, J.D., Gautam, R., Vergassola, M., and Murthy, V.N. (2019). Antagonistic odor interactions in olfactory sensory neurons are widespread in freely breathing mice | bioRxiv.

Zhan, C., and Luo, M. (2010). Diverse Patterns of Odor Representation by Neurons in the Anterior Piriform Cortex of Awake Mice. J. Neurosci. *30*, 16662–16672.